Pseudo-merohedral crystalline family of Ln-MOFs: relationship between the structure and the catalytic properties.

Richard F. D'Vries,[a] Natalia Snejko,[a] Marta Iglesias,[a] Enrique Gutiérrez-Puebla, [a] and M. Angeles Monge[a]*

Supporting Information

Section S1. Table Selected bond lengths [Å] and angles [º] for **RPF-20-**Eu, Gd and Er.

Section S2. Experimental X-ray powder patterns for **RPF-20**-Ln compounds.

Section S3. X-ray powder thermo-diffraction patterns for **RPF-20**-Eu.

Section S4. X-ray powder patterns for **RPF-20**-Ln compounds after TG analysis.

Section S5. X-ray powder patterns for **RPF-20**-Ln (Sm, Dy and Yb) before and after catalytic reactions.

Section S6. DSC analysis for the compound RPF-20-Yb before and after catalytic reaction.

Section S7. Comparison of catalytic profiles of the compound RPF-20-Yb dry, RPF-20-Yb and RPF-20-Yb 2^{do} cycle.

Section S8. TG analysis for the RPF-20-Ln compounds.

Section S1. Table Selected bond lengths [Å] and angles [º] for **RPF-20-**Eu, Gd and Er.

RPF-20-Eu		**RPF-20-Gd**		**RPF-20-Er**	
Eu1-N1	2.5785(117)	Gd1-N1	2.5276(145)	Er1-N1	2.4549(171)
Eu1-N2	2.5230(410)	Gd1-N2	2.5436(158)	Er1-N2	2.4965(163)
Eu1-O1	2.4519(95)	Gd1-O1	2.2995(149)	Er1-O1	2.3179(164)
Eu1-O10	2.3500(102)	Gd1-O10	2.4592(128)	Er1-O10	2.4681(170)
Eu1-O13	2.3892(95)	Gd1-O13	2.4384(126)	Er1-O13	2.3834(141)
Eu1-O14	2.4089(104)	Gd1-O14	2.3765(152)	E1-O14	2.3471(145)
Eu1-O19	2.3543(109)	Gd1-O19	2.2980(140)	Er1-O19	2.3191(158)
Eu2-N3	2.5539(107)	Gd2-N3	2.5305(162)	Er2-N3	2.4958(165)
Eu2-N4	2.5544(103)	Gd2-N4	2.5659(151)	Er2-N4	2.4948(177)
Eu2-O4	2.3738(103)	Gd2-O4	2.4413(131)	Er2-O4	2.4223(183)
Eu2-O7	2.4119(139)	Gd2-O7	2.3391(149)	Er2-O7	2.3178(164)
Eu2-O15	2.3969(102)	Gd2-O15	2.4153(142)	Er2-O15	2.3946(143)
Eu2-O16	2.4561(95)	Gd2-O16	2.3732(129)	E2-O16	2.3445(139)
Eu2-O20	2.3614(103)	Gd2-O20	2.3569(155)	Er2-O20	2.2521(174)
N1-Eu1-N2	64.39(36)	N1-Gd1-N2	64.46(49)	N1-Er1-N2	66.14 (54)
N1- Eu1-O1	81.39(34)	N1- Gd1-O1	127.58 (50)	N1- Er1-O1	130.98(56)
N1-Eu1-	160.07(36)	N1- Gd1-O14	80.53 (49)	N1-Er1-O14	79.31(53)
N2-Eu1-	80.85(33)	N2- Gd1-O13	162.66 (46)	N2-Er1-O13	132.41(52)
O1-Eu1-	130.49(34)	O1- Gd1-O10	139.27 (48)	O1-Er1-O10	136.95(58)
N3-Eu2-N4	64.26(34)	N3- Gd2-N4	65.09 (51)	N3-Er2-N4	66.50(58)
N3-Eu2-O4	79.36(35)	N3- Gd2-O4	80.16 (46)	N3-Er2-O4	71.73 (58)
N3-Eu2-	142.15(34)	N3- Gd2-O15	133.43 (51)	N3-Er2-O15	133.73(52)
O4-Eu2-	136.44(35)	O4- Gd2-O15	112.31 (46)	O4-Er2-O15	111.73(58)
O7-Eu2-	148.10(40)	O7- Gd2-O20	72.42 (50)	O7-Er2-O20	74.49(58)

Section S2. Experimental X-ray powder patterns for **RPF-20**-Ln compounds.

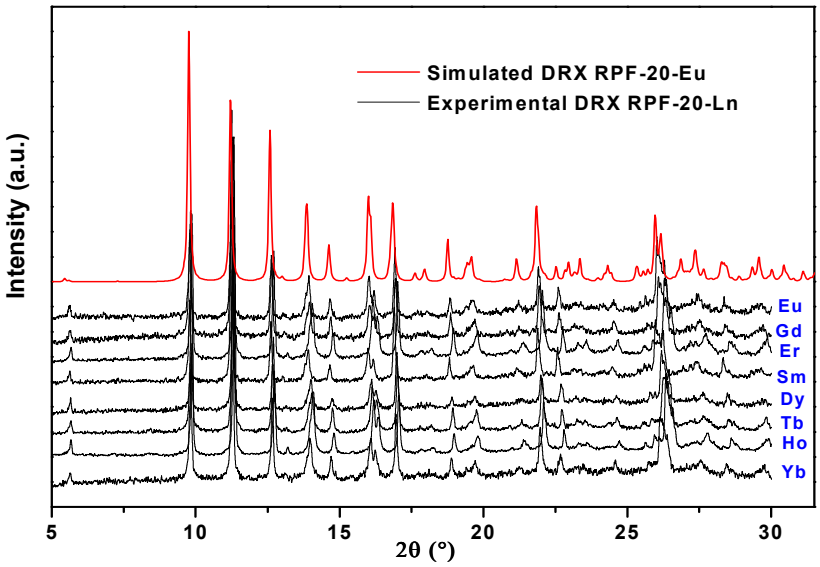

Section S3. X-ray powder thermo-diffraction patterns for **RPF-20**-Eu.

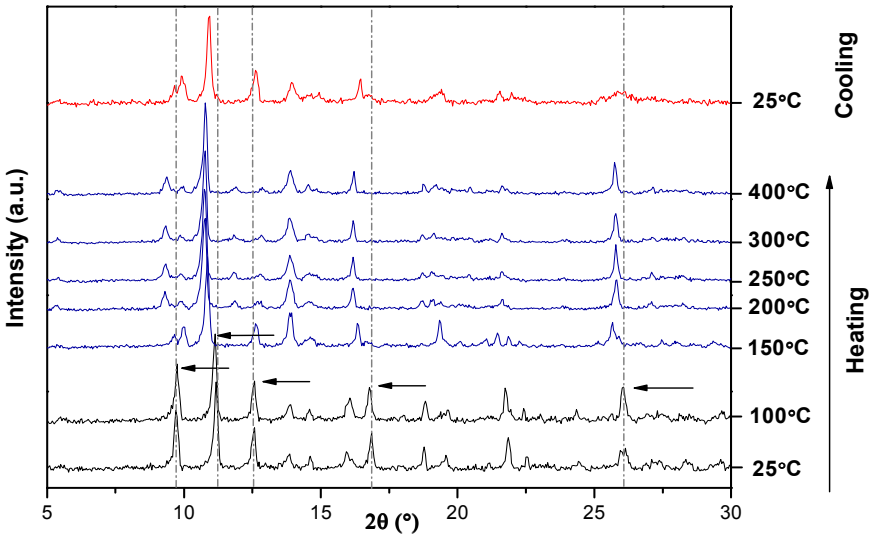

Section S4. X-ray powder patterns for **RPF-20**-Ln compounds after TG analysis.

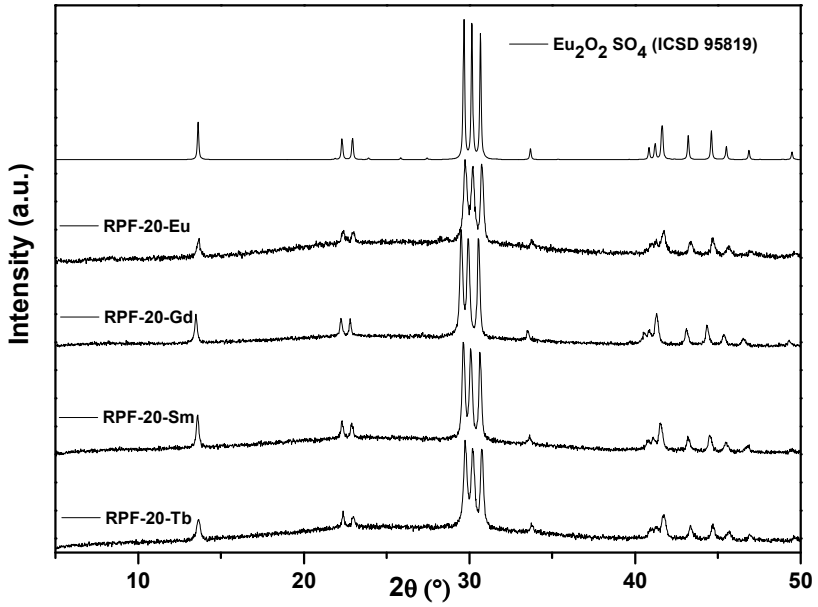

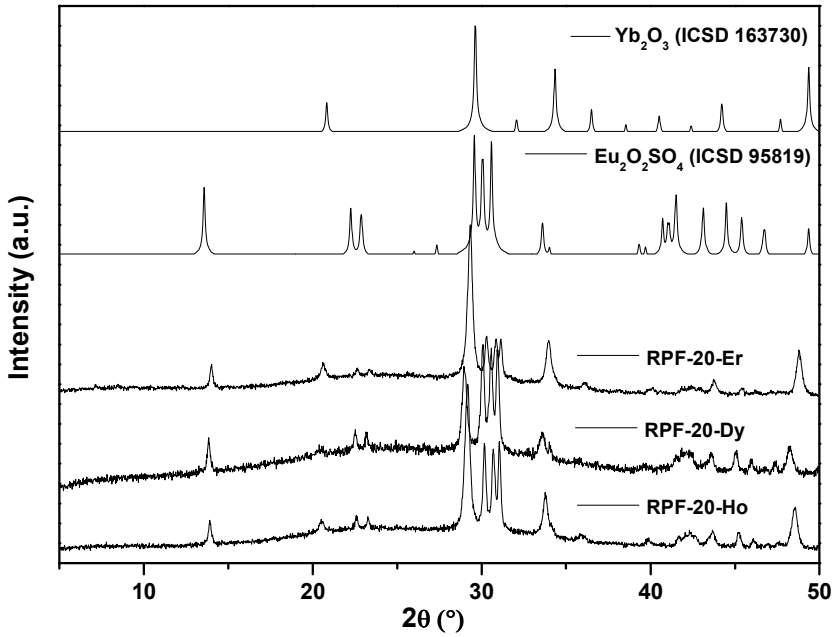

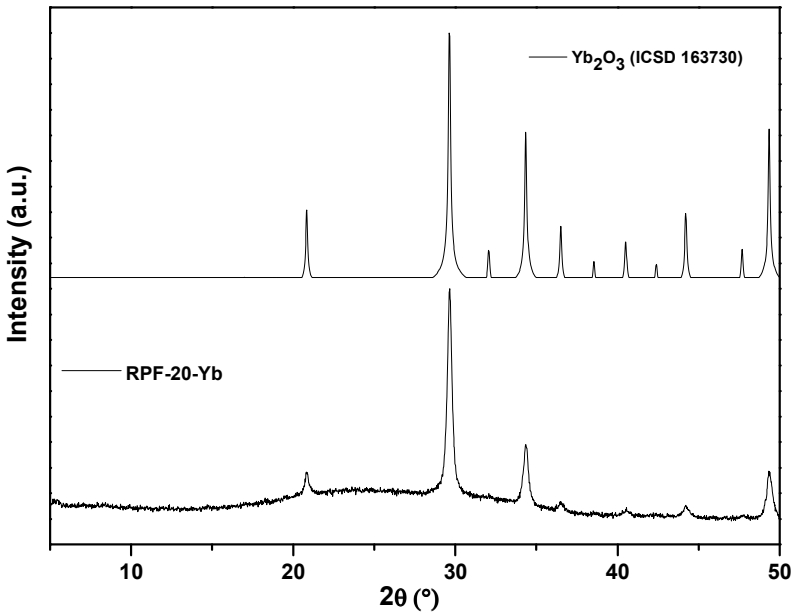

Section S5. X-ray powder patterns for **RPF-20**-Ln (Sm, Dy and Yb) before and after catalytic reactions.

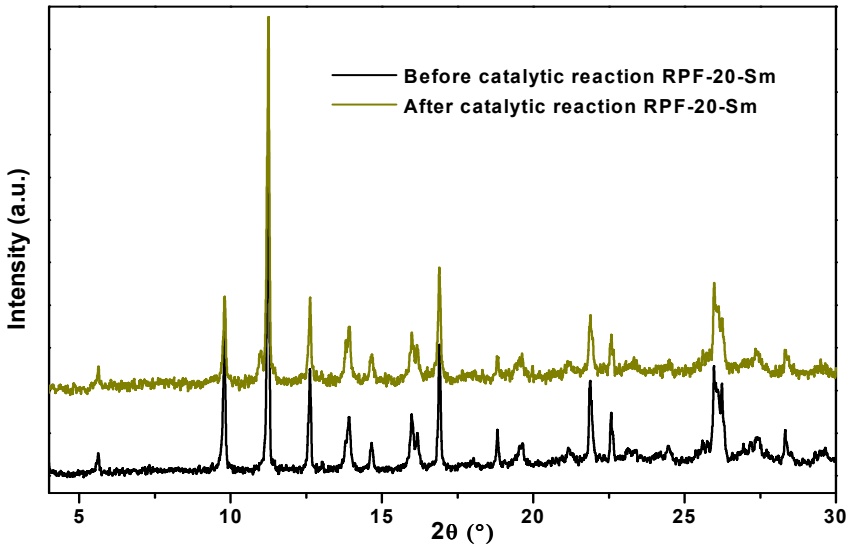

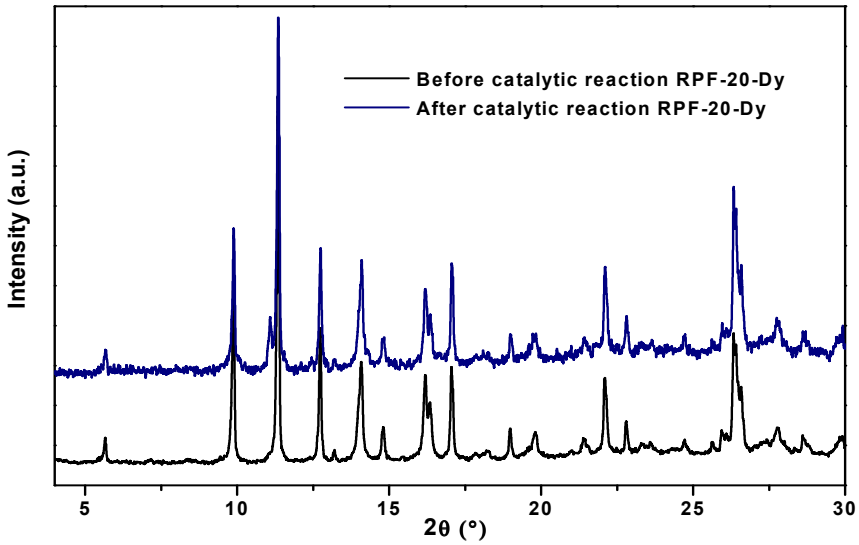
Before catalytic reaction RPF-20-Dy
After catalytic reaction RPF-20-Dy
Intensity (a.u.)
5
10
15
20
25
30
2θ (°)

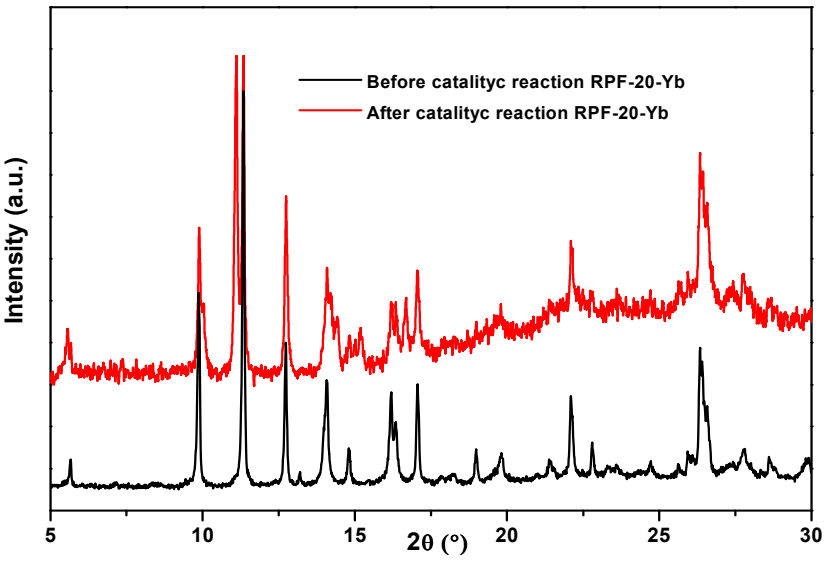
Before catalityc reaction RPF-20-Yb
After catalityc reaction RPF-20-Yb
Intensity (a.u.)
5
10
15
20
25
30
2θ (°)

Section S6. DSC analysis for the compound RPF-20-Yb before and after catalytic reaction.

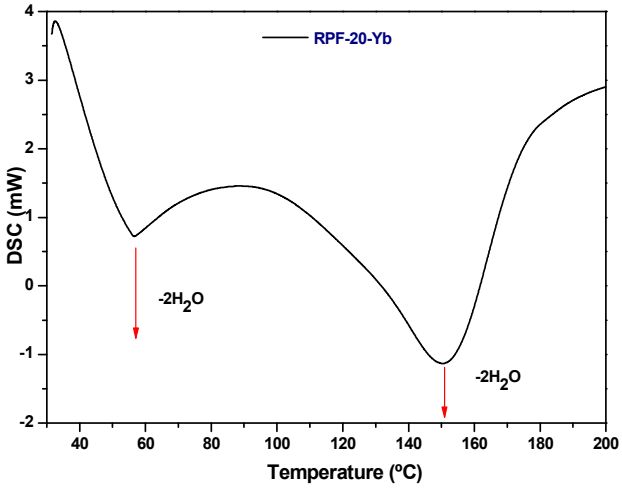

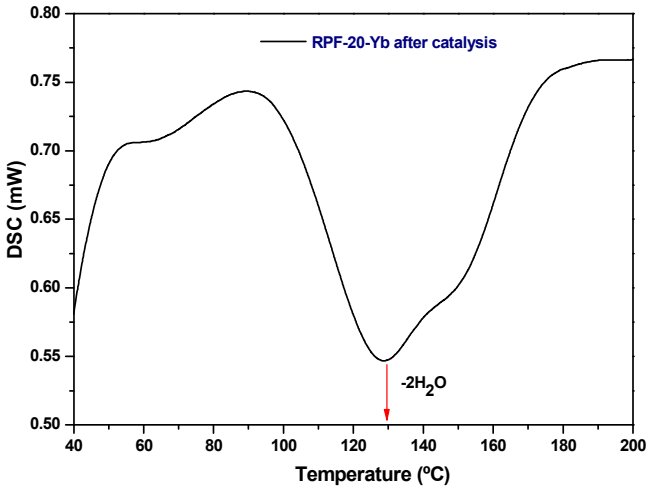

Section S7. Comparison of catalytic profiles of the compound RPF-20-Yb dry, RPF-20-Yb and RPF-20-Yb 2do cycle.

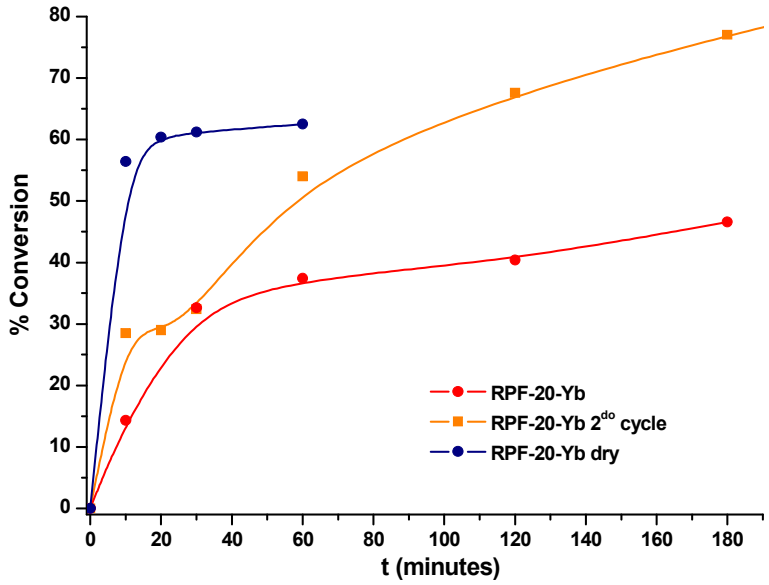

Section S8. TG analysis for the RPF-20-Ln compounds. Differences in the final decomposition compounds are due to the products different proportion in the mixtures of metallic oxides and oxysulfates, depending on the metal size.